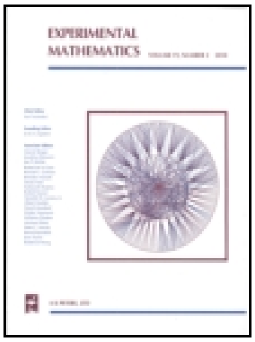

Experimental Mathematics

ISSN: 1058-6458 (Print) 1944-950X (Online) Journal homepage: https://www.tandfonline.com/loi/uexm20

A Census of Tetrahedral Hyperbolic Manifolds

Evgeny Fominykh, Stavros Garoufalidis, Matthias Goerner, Vladimir Tarkaev & Andrei Vesnin

To cite this article: Evgeny Fominykh, Stavros Garoufalidis, Matthias Goerner, Vladimir Tarkaev & Andrei Vesnin (2016) A Census of Tetrahedral Hyperbolic Manifolds, Experimental Mathematics, 25:4, 466-481, DOI: 10.1080/10586458.2015.1114436

To link to this article: https://doi.org/10.1080/10586458.2015.1114436

Published online: 06 Apr 2016.

EXPERIMENTAL MATHEMATICS
2016, VOL. 25, NO. 4, 466–481
http://dx.doi.org/10.1080/10586458.2015.1114436

A Census of Tetrahedral Hyperbolic Manifolds

Evgeny Fominykh[a,b], Stavros Garoufalidis[c], Matthias Goerner[d], Vladimir Tarkaev[a], and Andrei Vesnin[e]

[a]Laboratory of Quantum Topology, Chelyabinsk State University, Chelyabinsk, Russia; [b]Institute of Mathematics and Mechanics, Ekaterinburg, Russia; [c]School of Mathematics, Georgia Institute of Technology, Atlanta, GA, USA; [d]Pixar Animation Studios, Emeryville, CA, USA; [e]Sobolev Institute of Mathematics, Siberian Branch of the Russian Academy of Sciences, Novosibirsk, Russia

ABSTRACT
We call a cusped hyperbolic 3-manifold *tetrahedral* if it can be decomposed into regular ideal tetrahedra. Following an earlier publication by three of the authors, we give a census of all tetrahedral manifolds and all of their combinatorial tetrahedral tessellations with at most 25 (orientable case) and 21 (non-orientable case) tetrahedra. Our isometry classification uses certified canonical cell decompositions (based on work by Dunfield, Hoffman, and Licata) and isomorphism signatures (an improvement of dehydration sequences by Burton). The tetrahedral census comes in `Regina` as well as `SnapPy` format, and we illustrate its features.

KEYWORDS
hyperbolic 3-manifolds; regular ideal tetrahedron; census; tetrahedral manifolds; Bianchi orbifolds

2000 AMS SUBJECT CLASSIFICATION
Primary 57N10; Secondary 57M25

1. Introduction

1.1. Tetrahedral manifolds

We call a cusped hyperbolic 3-manifold *tetrahedral* if it can be decomposed into regular ideal tetrahedra. The combinatorial data of this decomposition is captured in the *combinatorial tetrahedral tessellation* which can be defined simply as an ideal triangulation where all edges have order 6. By Mostow rigidity, a combinatorial tetrahedral tessellation determines a tetrahedral manifold. However, there might be several non-isomorphic (i.e., not related by just relabeling tetrahedra and vertices) combinatorial tetrahedral tessellations yielding the same tetrahedral manifold. That is why we introduce the two terms tetrahedral manifold and combinatorial tetrahedral tessellation to distinguish whether we regard isometric or combinatorially isomorphic objects as equivalent.

The tetrahedral manifold were also called *maximum volume* in [Anisov 05, Vesnin et al. 11, Vesnin et al. 14, Vesnin et al. 15] because they are precisely the ones with maximal volume among all hyperbolic manifolds with a fixed number of tetrahedra. Thus, they also appear at the trailing ends of the `SnapPy` [Culler et al. 14] census manifolds sharing the same letter[1] (e.g., `m405` to `m412`, `s955` to `s961`, `v3551`, `t12833` to `t12845`, `o9_44249`). Moreover, the number of tetrahedra and the Matveev complexity [Matveev 03] also coincides for these manifolds.

The census of tetrahedral manifolds illustrates a number of phenomena of arithmetic hyperbolic manifolds including symmetries visible in the canonical cell decomposition but hidden by the combinatorial tetrahedral tessellation. In particular, the canonical cell decomposition might have non-tetrahedral cells.

Several manifolds that have played a key role in the development of hyperbolic geometry are tetrahedral, e.g., the complements of the figure-eight knot, the minimally twisted 5-chain link (which conjecturally is also the minimum volume orientable hyperbolic manifold with 5 cusps), and the Thurston congruence link. The last two have the special property that their combinatorial tetrahedral tessellation is maximally symmetric, i.e., any tetrahedron can be taken to any other tetrahedron in every orientation-preserving configuration via a combinatorial isomorphism. One of the authors has classified link complements with this special property in previous work [Goerner 15a].

We also construct several new links with tetrahedral complement.

1.2. Our results and methods

Our main goals (see [Goerner 15b] for the data) are the creation of

(a) The census of combinatorial tetrahedral tessellations up to 25 (orientable case), respectively, 21 (non-orientable case) tetrahedra.

CONTACT Stavros Garoufalidis stavros@math.gatech.edu School of Mathematics, Georgia Institute of Technology, Atlanta, GA 30332-0160, USA.
Color versions of one or more of the figures in the article can be found online at www.tandfonline.com/uexm
[1]The case of the letter `m` is exceptional because it spans several number of tetrahedra for purely historic reasons.

Table 1. Number of triangulations in the census.

Tetrahedra	Combinatorial tet. tessellations		Tetrahedral manifolds		Homology links
	Orientable	Non-or.	Orientable	Non-or.	
1	0	1	0	1	0
2	2	2	2	1	1
3	0	1	0	1	0
4	4	4	4	2	2
5	2	12	2	8	0
6	7	14	7	10	0
7	1	1	1	1	0
8	14	10	13	6	5
9	1	6	1	6	0
10	57	286	47	197	12
11	0	17	0	17	0
12	50	117	47	80	7
13	3	8	3	8	0
14	58	134	58	113	25
15	91	975	81	822	0
16	102	175	96	142	32
17	8	52	8	52	0
18	213	1118	199	810	66
19	25	326	25	326	0
20	1886	26,320	1684	22,340	209
21	31	251	31	251	0
22	390	–	381	–	148
23	58	–	58	–	0
24	1544	–	1465	–	378
25	7563	–	7367	–	0

(b) The grouping by isometry type and the corresponding canonical cell decompositions.
We ship this as a `Regina` [Burton 14] file containing triangulations in a hierarchy reflecting the grouping.

(c) The corresponding census of tetrahedral manifolds.
We ship this as a `SnapPy` census containing a representative triangulation for each isometry type. This census can be used just like any other `SnapPy` census.

(d) The list of covering maps between the combinatorial tetrahedral tessellations.

For (a), we use a new approach differing from the traditional one that starts by enumerating 4-valent graphs used first by Callahan–Hildebrand–Weeks [Callahan et al. 99] or variations of the traditional approach such as by Burton and Pettersson [Burton and Pettersson 14]. The advantage of our new approach is that it scales to a substantially higher number of tetrahedra because it allows for early pruning of triangulations with edges of wrong order. We also deploy isomorphism signatures to avoid recounting combinatorially isomorphic triangulations. Recall that the isomorphism signature is an improvement by Burton [Burton 11] of the (non-canonical) dehydration sequences. It is a complete invariant of the combinatorial isomorphism type of a triangulation. Algorithms 1 and 2 used for the enumeration of combinatorial tetrahedral tessellations are described in Section 2. Isomorphism signatures of orientable combinatorial tetrahedral tessellations with at most seven tetrahedra are presented in Table 2.

For (b), we use a new invariant we call the *isometry signature* (see Section 3). It is a complete invariant of the isometry type of a cusped hyperbolic 3-manifold. It is defined as the isomorphism signature of the canonical retriangulation of the canonical cell decomposition [Epstein and Penner 88]. To compute it, we use exact arithmetic to certify the canonical cell decomposition even when the cells are not tetrahedral, expanding on work by Dunfield, Hoffman, and Licata [Dunfield et al. 14].

For (d), we wrote a script that finds combinatorial homomorphisms from a triangulation to another triangulation.

Several of the techniques here are new and can be generalized: the *isometry signature* is an invariant that is defined for any finite-volume cusped hyperbolic 3-manifolds. It is a complete isometry invariant (and thus by Mostow rigidity a complete homotopy invariant) that can be effectively computed and, in general, be certified whenever the manifold is orientable and the canonical cell decomposition contains only tetrahedral cells using `hikmot` [Hoffman et al. 13]. We also provide an improvement of the code provided in [Dunfield et al. 14] to certify canonical triangulations that is simpler and generalizes to any number of cusps.

Applying the above discussed methods we obtain the following result.

Theorem 1.1. *The number of combinatorial tetrahedral tessellations and tetrahedral manifolds up to 25 tetrahedra for orientable manifolds and up to 21 tetrahedra for non-orientable manifolds are listed in Table 1 .*

Table 2. Isomorphism signatures for all orientable combinatorial tetrahedral tessellations with $n \leq 7$ tetrahedra.

n	Signature	Name	n	Signature	Name
2	`cPcbbbdxm`	otet02_{0000}	6	`gLLPQccdfeefqjsqqjj`	otet06_{0000}
2	`cPcbbbiht`	otet02_{0001}	6	`gLLPQccdfeffqjsqqsj`	otet06_{0001}
4	`eLMkbbdddemdxi`	otet04_{0000}	6	`gLLPQceefeffpupuupa`	otet06_{0002}
4	`eLMkbcddddedde`	otet04_{0001}	6	`gLMzQbcdefffhxqqxha`	otet06_{0003}
4	`eLMkbcdddhxqdu`	otet04_{0002}	6	`gLMzQbcdefffhxqqxxq`	otet06_{0004}
4	`eLMkbcdddhxqlm`	otet04_{0003}	6	`gLvQQadfedefjqqasjj`	otet06_{0005}
5	`fLLQcbcedeeloxset`	otet05_{0000}	6	`gLvQQbefeeffedimipt`	otet06_{0006}
5	`fLLQcbdeedemnamjp`	otet05_{0001}	7	`hLvAQkadfdgggfjxqnjnbw`	otet07_{0000}

```
Function FindAllTetrahedralTessellations(integer max, bool orientable)
    Result: Returns all (non-)orientable tetrahedral tessellations up to combinatorial isomorphism with at most max tetrahedra.
    result ← {} ;                                              /* resulting triangulations */
    already_seen ← {} ;                        /* isomorphism signatures encounteredearlier */

    Procedure RecursiveFind(Triangulation t)
        Result: Searches all triangulations obtained from t by gluing faces or adding tetrahedra.
        /* Close order 6 edges and reject unsuitable triangulations                         */
        if FixEdges(t) = "valid" then
            /* Skip triangulations already seen earlier                                     */
            if isomorphismSignature(t) ∉ already_seen then
                already_seen ← already_seen ∪ {isomorphismSignature(t)};
                if t has no open faces then
                    /* t orientable by construction if orientable = true                    */
                    if t is non-orientable or orientable = true then
                        result ← result ∪ {t};
                    end
                else
                    /* This choice results in faster enumeration                            */
                    choose an open face F1=(tetrahedron, f1) of t adjacent to an open edge of highest order;
                    if t has less than max tetrahedra then
                        ResursiveFind(t with a new tetrahedron glued to F1 via an odd permutation)
                    end
                    for each open face F2 ≠ F1 of t do
                        for each p ∈ S4 do
                            if p(f1) = f2 then
                                if p is odd or orientable = false then
                                    RecursiveFind(t with F1 glued to F2 via p);
                                end
                            end
                        end
                    end
                end
            end
        end
    end
    RecursiveFind(triangulation with one unglued tetrahedron);
    return result
end
```

Algorithm 1: The main function to enumerate all tetrahedral tessellations.

All combinatorial tetrahedral tessellations and tetrahedral manifolds indicated in Table 1 are enumerated in supplement files available in [Goerner 15b].

Knots and links with tetrahedral complement are shown in Figures 3–5.

1.3. Features of the tetrahedral census

Properties of tetrahedral manifolds that make them interesting to study include:

- The tetrahedral manifolds are arithmetic as they are a proper subset of the commensurability class of figure-eight knot complement, closed under finite coverings, see Section 5.2.
- The tetrahedral manifolds are exactly those with maximal volume among all cusped hyperbolic manifolds with a fixed number of tetrahedra.
- Their Matveev complexity equals the number of regular ideal tetrahedra.
- Many combinatorial tetrahedral tessellations hide symmetries, i.e., there are isometries of the corresponding tetrahedral manifold that are not induced from a combinatorial isomorphism of the combinatorial tetrahedral tessellation.
- A substantial fraction of tetrahedral manifolds are link complements.

2. The enumeration of combinatorial tetrahedral tessellations

We use Algorithm 1 to enumerate the combinatorial tetrahedral tessellations. The input is the maximal number of tetrahedra to be considered and a flag indicating whether we wish to enumerate the orientable or the non-orientable tessellations. The result is a set of ideal triangulations where each edge has order 6 resulting in manifolds of the desired orientability.

As pointed out in Section 1 our algorithm differs from the traditional approach: we recursively try all possible ways open faces can be face-paired without enumerating 4-valent graphs first. This will, of course, result in many duplicates, so we keep a set of isomorphism signatures (see [Burton 11]) of previously encountered triangulations around to prevent recounting. Recall that an isomorphism signature is, unlike a dehydration sequence, a complete invariant of the combinatorial isomorphism type of a triangulation.

The advantage of this approach is that we can insert a procedure that can prune the search space early on. In our case, this procedure is given in Algorithm 2 and rejects ideal triangulations where edges have the wrong order. It also rejects ideal triangulations with non-manifold topology. These can occur when the tetrahedra around an edge cannot be oriented consistently and the vertex link of the center of the edge becomes a projective plane $\mathbb{RP}^2$.

Function `FixEdges(`*Triangulation t*`)`
  Result: t is modified in place. Returns "valid" or "invalid".
  While *t has open edge e of order 6*
    close edge *e*;
  return *"valid" if every edge e*
   - *has order < 6 (if open) or $= 6$ (if closed) and*
   - *has no projective plane as vertex link.*

end

Algorithm 2: A helper function closing order 6 edges and rejecting triangulations which cannot result in tetrahedral tessellations.

The algorithm has been implemented using `Regina` and we briefly recall how a triangulation is presented. The vertices of each tetrahedron are indexed 0, 1, 2, 3 and the faces are indexed by the number of the vertex opposite to it. Triangulations in intermediate stages will have unpaired faces. We call a face open if it is unpaired, otherwise closed. A triangulation consists of a number of tetrahedra and for each tetrahedron T_1 and each face index $f_1 = 0, ..., 3$, we store two pieces of data to encode whether and how the face $F_1 = (T_1, f_1)$ is glued to another face $F_2 = (T_2, f_2)$ with face index f_2 of another (not necessarily distinct) tetrahedron T_2:

(1) A pointer to T_2. If F_1 is an open face, this pointer is null.
(2) An element $p \in S_4$ such that $p(f_1) = f_2$ and the vertex $i \neq f_1$ of T_1 is glued to $p(i)$ of T_2.

The face pairings implicitly determine edge classes. We call such an edge open if it is adjacent to an open face (necessarily so exactly two) and otherwise closed. Closing an open edge means gluing the two open adjacent faces by the suitable permutation.

The source for the implementation is in `src/genIsomoSigsOfTetrahedralTessellations.cpp`. Table 2 lists a small selection of the resulting combinatorial tetrahedral tessellations as isomorphism signatures. The complete list corresponding to Table 1 is available at [Goerner, data/], also see Section 4.

3. The isometry signature

In the previous section, we enumerated all combinatorial tetrahedral tessellations with a given maximal number of tetrahedra up to combinatorial isomorphism. In the next step, we want to find the equivalence classes of those combinatorial tetrahedral tessellations yielding the same tetrahedral manifold up to isometry.

We do this by grouping combinatorial tetrahedral tessellations by their *isometry signature* which we define, compute, and certify in this section. To summarize, the isometry signature is the isomorphism signature of the canonical retriangulation of the canonical cell decomposition. If, however, the canonical cell decomposition has simplices as cells, we short-circuit and just use the isomorphism signature of the canonical cell decomposition itself. We can certify the isometry signature by using exact computations to determine which faces in the proto-canonical triangulation are transparent.

The code implementing the certified canonical retriangulation can be found in `src/canonical_o3.py`. The code to group (and name) the combinatorial tetrahedral tessellations by isometry signature is in `src/identifyAndNameIsometricIsomoSigsOfTetrahedralTessellations.py`.

3.1. Definition

Recall that the hyperboloid model of 3-dimensional hyperbolic space $\mathbb{H}^3$ in $(3 + 1)$-Minkowski space (with inner product defined by $\langle x, y\rangle = x_0y_0 + x_1y_1 + x_2y_2 - x_3y_3$) is given by

$$S^+ = \{x = (x_0, ..., x_3) \mid x_3 > 0, \quad \langle x, x\rangle = -1\}.$$

For a cusped hyperbolic manifold M, choose a horotorus cusp neighborhood of the same volume for each cusp. Lift M and the cusp neighborhoods to $\mathbb{H}^3 \cong S^+$. The cusp neighborhoods lift to a $\pi_1(M)$-invariant set of horoballs. For each horoball $B \subset S^+$, there is a dual vector v_B that is light-like (i.e., $\langle v_B, v_B\rangle = 0$) and such that $w \in B \Leftrightarrow \langle v_B, w\rangle > -1$. The boundary of the convex hull of all v_B has polygonal faces.

Definition 3.1. The *canonical cell decomposition* of M is given by the radial projection of the polygonal faces of the boundary of the convex hull of all v_B onto S^+.

The canonical cell decomposition was introduced by Epstein and Penner [Epstein and Penner 88]. It does not depend on a particular choice of cusp neighborhoods as long as they all have the same volume, or equivalently, same area.

Definition 3.2. A triangulation which is obtained by subdividing the cells of the canonical cell decomposition and inserting (if necessary) flat tetrahedra is called a *proto-canonical triangulation*. If it contains no flat tetrahedra, i.e., all tetrahedra are positively oriented, it is called a *geometric proto-canonical triangulation*.

The result of calling `canonize` on a `SnapPy` manifold is a proto-canonical triangulation. If the canonical cell decomposition has cells which are not ideal tetrahedra (non-regular or regular), there might be more than one proto-canonical triangulation of the same manifold. A face of a proto-canonical triangulation which is part of a 2-cell of the canonical cell decomposition is called *opaque*. Otherwise, a face is called *transparent*.

Definition 3.3. Consider a 2-cell in the canonical cell decomposition which is an n-gon. Pick the suspension of such an n-gon by the centers of the two neighboring 3-cells. These suspensions over all 2-cells form a decomposition of M into topological diamonds. Each diamond can be split into n tetrahedra along its central axis. The result is called the *canonical retriangulation*.

The canonical retriangulation carries exactly the same information as the canonical cell decomposition (just packaged as a triangulation) and thus only depends on (and uniquely determines) the isometry type of the manifold. `SnapPy` uses it internally to compute, for example, the symmetry group of a hyperbolic manifold M by enumerating the combinatorial isomorphisms of the canonical retriangulation of M. Similarly, `SnapPy` uses it to check whether two manifolds are isometric.

Definition 3.4. The *isometry signature* of M is the isomorphism signature of the canonical retriangulation if the canonical cell decomposition has non-simplicial cells. Otherwise, it is the isomorphism signature of the canonical cell decomposition itself.

Example 3.5. The triangulation of `m004` given in the `SnapPy` census already is the canonical cell decomposition. Thus, the isometry signature of the manifold `m004` is the isomorphism signature of the census triangulation, namely `cPcbbbiht` presented in Table 2. In the census of tetrahedral hyperbolic manifolds `m004` named otet02_{0001}. Recall that this manifold is the figure-eight knot complement.

The cell decomposition for `m202` given in the `SnapPy` census is not canonical. The isomorphism signature of its `SnapPy` triangulation is `eLMkbbdddemdxi` presented in Table 2. In the census of tetrahedral hyperbolic manifolds `m202` named otet04_{0000}. Observe, that otet04_{0000} is the complement of a 2-component link presented in Figure 3. The isometry signature of `m202` is `jLLzzQQccdffihhiiqffofafoaa` that is realized by a triangulation with 10 tetrahedra.

3.2. Computation of the tilt

Consider an ideal triangulation $\mathcal{T} = \cup_i T_i$ of a cusped manifold M with a shape assignment for each tetrahedron, i.e., a $z_i \in \mathbb{C} \setminus \{0, 1\}$ determining an embedding of the tetrahedron T_i as ideal tetrahedron in $\mathbb{H}^3$ up to isometry. If the shapes fulfill the consistency equations (also known as gluing equations) in logarithmic form and have positive imaginary parts, we call the triangulation together with the shape assignment a *geometric ideal triangulation*. Thurston shows that a geometric ideal triangulation glues up to a complete hyperbolic structure on M. Given a geometric ideal triangulation and a face F of it, the tilt $\text{Tilt}(F)$ is a real number defined by Weeks [Weeks 93] which determines whether a given triangulation is proto-canonical and which faces are transparent.

We now describe how to compute $\text{Tilt}(F)$ following the notation in [Dunfield et al. 14] and use it to determine the canonical retriangulation.

3.2.1. Computation of a cusp cross section

The ideal tetrahedra intersect the boundary of a neighborhood of a cusp in Euclidean triangles and we call the resulting assignment of lengths to edges a *cusp cross section*. We first compute a cusp cross section C_c for some neighborhood of each cusp c by picking an edge e_j for each cusp and assigning length $e_j = 1$ to it. We recursively assign lengths to the other edges by using that the ratio of two edge lengths is given by the respective $|z_i^*|$ where z_i^* is one of the edge parameters z_i, $z_i' = \frac{1}{1-z_i}$, $z_i'' = 1 - \frac{1}{z_i}$:

$$e_l = e_k \cdot |z_i^*|.$$

3.2.2. Computation of the cusp area

We can compute the area of each Euclidean triangle t as

$$A(t) = \frac{1}{2} e_k^2 \cdot \text{Im}(z_i^*),$$

where e_k and z_i^* are as above. The cusp area $A(C_c)$ of the cusp cross section C_c is simply the sum of the areas $A(t)$ over all its Euclidean triangles t.

3.2.3. Normalization of the cusp area

We need to scale each cusp cross section to have the same target area A. The new edge lengths and areas are given by

$$e'_l = e_l \cdot \sqrt{\frac{A}{A(C_c)}} \quad \text{and} \quad A'(t) = A(t)\frac{A}{A(C_c)}.$$

3.2.4. Computation of the circumradius for each Euclidean triangle

Let R^i_v denote the circumradius of the Euclidean triangle t that is the cross section of the tetrahedron i near vertex $v \in \{0, 1, 2, 3\}$. If e'_j, e'_k, and e'_l are the edge lengths of t, elementary trigonometry implies

$$R^i_v = \frac{e'_j e'_k e'_l}{4A'(t)}.$$

3.2.5. Computation of the tilt of a vertex

Compute

$$\mathrm{Tilt}(i, v) = R^i_v - \sum_{u \neq v} R^i_u \frac{\mathrm{Re}(z^*_i)}{|z^*_i|}, \tag{3–1}$$

where z^*_i is the edge parameter for the edge from u to v.

3.2.6. Computation of the tilt of a face

If the face F opposite to vertex v of tetrahedron i is glued to that opposite of v' of tetrahedron i', the tilt of the face is defined as

$$\mathrm{Tilt}(F) = \mathrm{Tilt}(i, v) + \mathrm{Tilt}(i', v').$$

3.2.7. Determination of transparent faces and canonical retriangulation

Weeks proves that [Weeks 93] a geometric ideal triangulation is a geometric proto-canonical triangulation if all $\mathrm{Tilt}(F) \leq 0$. In that case, a face F is transparent if and only if $\mathrm{Tilt}(F) = 0$.

`SnapPy` implements an algorithm to compute the canonical retriangulation. It can be refactored so that it takes as input the opacities of the faces and is purely combinatorial. In case of a geometric (!) proto-canonical triangulation, Weeks' arguments in the `SnapPy` code prove that this algorithm works correctly.

For all manifolds we encountered, several randomization trials were always sufficient to ensure that the ideal triangulation returned by `SnapPy`'s `canonize` is always geometric proto-canonical. Thus, the result of the purely combinatorial canonical retriangulation algorithm is known to be correct as long as we certify the input to be a geometric proto-canonical triangulation with certified opacities of its faces.

Remark 3.6. Even though we can certify the results for all listed manifolds in the tetrahedral census, it is not known if

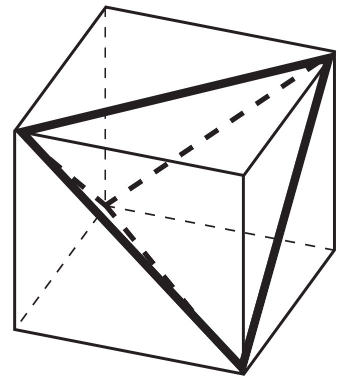

Figure 1. Subdivision of a cube into 5 tetrahedra. For a regular ideal hyperbolic cube, all tetrahedra are again regular ideal. The subdivision introduced additional diagonals on the faces.

- every cusped hyperbolic manifold has a geometric proto-canonical triangulation,
- every cusped hyperbolic manifold has a geometric ideal triangulation.

Moreover, it is known that `SnapPy`'s implementation can give the wrong canonical retriangulation if we use as input a non-geometric (!) proto-canonical triangulation. As pointed out by Burton, the triangulation `x101` in the non-orientable cusped `SnapPy` census is such an example where flat tetrahedra cause `SnapPy` to give an incorrect canonical retriangulation.

It is unclear to the authors which of the following factors contribute to the incorrect result:

- Numerical precision issues.
- `SnapPy`'s extension of the above definition of $\mathrm{Tilt}(F)$ to flat tetrahedra (where some $A(t) = 0$ and thus $R^i_v = \infty$) using `CIRCUMRADIUS_EPSILON`.
- Week's arguments for the purely combinatorial part of the canonical retriangulation algorithm seem to implicitly assume that there are no flat-tetrahedra.

The existence of geometric triangulations of a hyperbolic manifold can be proven when some tetrahedra are allowed to be flat [Petronio and Weeks 00]. It can also be proven virtually [Luo et al. 08].

Remark 3.7. Call a manifold that can be decomposed into regular ideal cubes *cubical*. Recall that a regular ideal cube can be subdivided into 5 regular ideal tetrahedra, see Figure 1. However, this does not imply that a cubical manifold is tetrahedral.

A counter-example is the manifold appearing in the census as `x101` and `x103`. Its canonical cell decomposition consists of one regular ideal cube. As Burton explained [Burton 14], `x101` subdivides the cube into 5 regular ideal tetrahedra but needs to insert a flat tetrahedron to match the diagonals on the cube. Thus, it is not a tetrahedral manifold (but still has a tetrahedral double-cover $\mathrm{ntet10}_{0093}$).

`x103` splits the same cube into 6 non-regular tetrahedra and is a geometric proto-canonical triangulation.

3.3. Certification for tetrahedral manifolds

Let $\sqrt{\mathbb{Q}^+}$ denote the multiplicative group of all square roots of positive rational numbers and let $\mathbb{Q}(\sqrt{\mathbb{Q}^+}) \subset \mathbb{C}$ be the field generated by $\sqrt{\mathbb{Q}^+}$.

Lemma 3.8. *If we pick as target area $A = \sqrt{3}$, we have for a geometric proto-canonical triangulation of a tetrahedral manifold M:*

$$z_i^* \in \mathbb{Q}(\sqrt{-3}); \qquad A(C_c) \in \mathbb{Q}^+\sqrt{3};$$
$$|z_i^*|, e_l, A(t), e_l', A'(t), R_v^i \in \sqrt{\mathbb{Q}^+};\ \mathrm{Tilt}(F) \in \mathbb{Q}(\sqrt{\mathbb{Q}^+}).$$

Proof. M and thus its universal cover can be decomposed into regular ideal tetrahedra. The resulting regular tessellation in $\mathbb{H}^3$ can be chosen to have vertices at $\mathbb{Q}(\sqrt{-3})$ (also see Section 5), thus the shapes of any ideal triangulation of M are in $\mathbb{Q}(\sqrt{-3})$.

Develop a cusp cross section constructed above in $\mathbb{C}$ such that the vertices of the edge set to length 1 are at 0 and 1. Then all vertices have complex coordinates in $\mathbb{Q}(\sqrt{-3})$ and a fundamental domain in $\mathbb{C}$ for the cusp is a parallelogram spanned by two complex numbers in $\mathbb{Q}(\sqrt{-3})$. The area $A(C_c)$ of such a parallelogram is in $\mathbb{Q}^+\sqrt{3}$.

The rest follows from the above formulas. □

We can represent a z_i^* exactly by $r_1 + r_2\sqrt{-3}$ with $r_1, r_2 \in \mathbb{Q}$. We can represent the other quantities exactly using Corollary 3.10 below.

Lemma 3.9. *Let $p_1, \ldots, p_r$ denote a list of distinct prime numbers and $K = \mathbb{Q}(\sqrt{p_1}, \ldots, \sqrt{p_r})$ denote the corresponding number field. Then,*

(a) $K/\mathbb{Q}$ is Galois with Galois group $G(K/\mathbb{Q}) = (\mathbb{Z}/2\mathbb{Z})^r$.

(b) If $\mathbb{Q} \subset L \subset K$ is a subfield of K such that $[L : \mathbb{Q}] = 2$ then $L = \mathbb{Q}(\sqrt{p_I})$ where $p_I = \prod_{i\in I} p_i$ for some nonempty $I \subset \{1, \ldots, r\}$.

(c) The $\mathbb{Q}$-linear map

$$\mathbb{Q}(\sqrt{p_1}) \otimes_{\mathbb{Q}} \mathbb{Q}(\sqrt{p_2}) \otimes_{\mathbb{Q}} \ldots \otimes_{\mathbb{Q}} \mathbb{Q}(\sqrt{p_r}) \to K,$$
$$x_1 \otimes \ldots \otimes x_r \mapsto \prod_{i=1}^{r} x_i$$

is an isomorphism of $\mathbb{Q}$-vector spaces.

Proof. We will prove this by induction on r. When $r = 1$ (a) is obvious and (b) follows from the fundamental theorem of Galois theory [Lang 02, VI,Thm.1.2].

Assume that the lemma is true for $r - 1$, and let $K_1 = \mathbb{Q}(\sqrt{p_1}, \ldots, \sqrt{p_{r-1}})$ and $K_2 = \mathbb{Q}(\sqrt{p_r})$. Then, we claim that $K_1 \cap K_2 = \mathbb{Q}$. Indeed, otherwise we have $K_2 \subset K_1$ and by part (b) it follows that $\mathbb{Q}(\sqrt{p_r}) = \mathbb{Q}(\sqrt{p_I})$ for some nonempty subset $I \subset \{1, \ldots, r-1\}$. So, $\sqrt{p_r} = a + b\sqrt{p_I}$ for $a, b \in \mathbb{Q}$. Squaring, we get

$$p_r = a^2 + b^2 p_I, \qquad ab = 0.$$

If $a = 0$ then $p_r = b^2 p_I$ and since I is nonempty, it follows that p_i^2 divides p_r where p_i, p_r are distinct primes, a contradiction. If $b = 0$ then $p_r = a^2$ and p_r is a prime number, also a contradiction. This shows that $K_1 \cap K_2 = \mathbb{Q}$. Let $K = K_1K_2 = \mathbb{Q}(\sqrt{p_1}, \ldots, \sqrt{p_r})$ denote the composite field. It follows by [Lang 02, VI,Thm.1.14] that K is a Galois extension with Galois group $G(K/\mathbb{Q}) = G(K_1/\mathbb{Q}) \times G(K_2/\mathbb{Q}) = (\mathbb{Z}/2\mathbb{Z})^r$. This proves part (a) of the inductive part. Part (b) follows from part (a) by the fundamental theorem of Galois theory [Lang 02, VI,Thm.1.2] and the classification of all index 2 subgroups of $(\mathbb{Z}/2\mathbb{Z})^r$. Part (c) follows from part (a) and the induction hypothesis. □

Part (c) of Lemma 3.9 implies the following corollary.

Corollary 3.10. *Every element in $\mathbb{Q}(\sqrt{\mathbb{Q}^+})$ has a unique representative of the form*

$$r_1\sqrt{n_1} + \ldots + r_k\sqrt{n_k}, \tag{3–2}$$

where $r_i \in \mathbb{Q} \setminus 0$ and $n_1 < \ldots < n_k$ are square-free positive integers.

Remark 3.11. For the purpose of effective exact computation, we need an explicit way of adding, subtracting, multiplying, and dividing expressions of the form (3–2). This is obvious except for division where we give the following algorithm: to compute n/d where n and d are two such forms and d contains a non-rational term $r_j\sqrt{n_j}$, pick a prime p dividing n_j. We can write d as $d_0 + \sqrt{p}d_1$ such that d_0 contains no term $r_i\sqrt{n_i}$ with $p|n_i$. We now have

$$\frac{n}{d} = \frac{n(d_0 - \sqrt{p}d_1)}{(d_0 + \sqrt{p}d_1)(d_0 - \sqrt{p}d_1)} = \frac{n(d_0 - \sqrt{p}d_1)}{d_0^2 - pd_1^2}.$$

The new denominator is simpler because it contains no more terms $r_i\sqrt{n_i}$ with $p|n_i$. Thus, by repeating this process we can eliminate all primes in the terms of the denominator.

When we say *using interval arithmetics*, we mean:

(1) We convert the exact representation of each quantity in $\mathbb{Q}(\sqrt{\mathbb{Q}^+})$, respectively, $\mathbb{Q}(\sqrt{-3})$ to an interval $[a, b]$, respectively, a complex interval $[a, b] + [a', b']i$. These intervals have interval semantics: the true value of the quantity is guaranteed to be contained in the interval.

(2) Any operations such as + or log are carried out such that interval semantics is preserved, i.e., the

resulting interval is again guaranteed to contain the true value of the computed quantity.

(3) An inequality involving an interval is considered certified only if it is true for all values in the interval, e.g., if the interval given for x is $[a, b]$, then $x < 0$ is certified only if $b < 0$.

We can now certify the geometric proto-canonical triangulation and the opacities of its faces. Our input is a candidate geometric proto-canonical triangulation obtained by calling `SnapPy`'s `canonize` on a tetrahedral manifold. We first guess exact values z_i from the approximated shapes reported by `SnapPy`. Using those guesses, we verify

(1) the rectangular form of the edge equations exactly,
(2) $\text{Im}(z_i) > 0$ for each tetrahedron (using interval arithmetics),
(3) $|e| < 10^{-7}$ for each edge where e is the error of the logarithmic form of the edge equation (using interval arithmetics),
(4) all the equations (Section 3.2.1) exactly,
(5) $\text{Tilt}(F) < 0$ (using interval arithmetics) for an opaque face, respectively, $\text{Tilt}(F) = 0$ (using exact arithmetics) for a transparent face.

(1) implies that the error in (3) will be a multiple of $2\pi i$ so a small enough error implies that the logarithmic form of the edge equations is fulfilled exactly. Together with (2), this means that the tetrahedra yield a (not necessarily complete) hyperbolic structure. Completeness is ensured by (4) which checks that the cusp cross section is Euclidean. Checking (4) really means verifying that the recursion process to obtain the edge lengths could construct a consistent result. (5) certifies the geometric proto-canonical triangulation and the opacities of the faces.

Remark 3.12. Note that in the process, we actually produce complex intervals for the shapes from `SnapPy`'s approximations certified to contain the true values. We can do this because we know that the shapes are in the field $\mathbb{Q}(\sqrt{-3})$ and thus can guess exact solutions and verify them exactly. An alternative method to obtain certified intervals from approximated shapes is the Krawczyk test implemented in `hikmot` [Hoffman et al. 13]. We could not use it here though, because it cannot deal with non-orientable manifolds. The edge equations for a non-orientable manifold are polynomials in z_i^* and $1/\bar{z}_i^*$.

Remark 3.13. We could have also avoided guessing by tracking `SnapPy`'s algorithm to obtain a proto-canonical triangulation. We know that the shapes of the tetrahedral tessellation are all exactly represented by $\frac{1}{2} + \frac{1}{2}\sqrt{-3}$ and that `SnapPy` is performing 2–3 and 3–2 moves during the algorithm. However, this would require changes to the `SnapPea` kernel since it does not report the sequence of moves it performed.

For guessing a rational representation from an approximation, we use the `fractions` module shipped with `python`. It essentially computes the continued fraction for a given real number and evaluates it at a stage where the resulting denominator is less than a given bound (10,000 in our case). For the (complex) interval arithmetics, we use `sage`. Our implementation in `python` is based on the script given in [Dunfield et al. 14].

3.4. Certification in the generic case

Dunfield, Hoffman, and Licata give an implementation in [Dunfield et al. 14] to certify a triangulation to be the canonical cell decomposition (which cannot contain non-tetrahedral cells). Though not needed here, we want to point out that their implementation can be both simplified and generalized to any number of cusps.

They start with certified complex intervals for the shapes returned by `hikmot` [Hoffman et al. 13]. But instead of following the complicated procedure in [Dunfield et al. 14, Section 3.7], one can simply apply interval arithmetics to the above equations to compute $\text{Tilt}(F)$. The result is an interval $[a, b]$ for each $\text{Tilt}(F)$ that is guaranteed to contain the true value of $\text{Tilt}(F)$. If $b < 0$ for each interval, then the $\text{Tilt}(F)$ are certified to be less than 0, thus the given ideal triangulation is the canonical cell decomposition.

We provide a version of `canonical.py` here that implements this.

4. Results of the implementation of algorithms

We implemented the algorithms described in the previous section, see [Goerner 15b] for the resulting data. The longest algorithm to run was the enumeration of the combinatorial tetrahedral tessellations: the orientable case up to 25 tetrahedra and the non-orientable one up to 21 tetrahedra each took about ≈6 weeks CPU time and ≈70 Gb of memory on a Xeon E5-2630, 2.3 Ghz. The number of resulting combinatorial tetrahedral tessellations and tetrahedral manifolds are listed in Table 1.

4.1. Names of tetrahedral manifolds

We give the tetrahedral manifolds names such as "otet08_{0002}" (orientable), respectively, "ntet02_{0000}" (non-orientable) with "tet" followed by the number of tetrahedra and an index. The different combinatorial tetrahedral tessellations corresponding to the same tetrahedral manifold are named with an additional index, e.g., "$\text{otet08}_{0002}\#0$" and "$\text{otet08}_{0002}\#1$." We choose as canonical representative for an isometry class the first combinatorial tetrahedral tessellation, e.g., $\text{otet08}_{0002}\#0$ for the tetrahedral manifold otet08_{0002}.

The indices are canonical: before indexing the combinatorial tetrahedral tessellations and tetrahedral manifolds, we first sort the combinatorial tetrahedral tessellations within an isometry class lexicographically by isomorphism signature and then sort the tetrahedral manifolds lexicographically by the isomorphism signature of their canonical representative.

4.2. SnapPy census

Our census of tetrahedral manifolds can be easily accessed from `SnapPy`. Simply change to the directory `snappy` accompanying this article and type `from tetrahedralCuspedCensus import *`. The two censuses `TetrahedralOrientableCuspedCensus` and `TetrahedralNonorientableCuspedCensus` have the same methods as any other census such as `OrientableCuspedCensus`. Here are examples of how to use them:

```
>>> from tetrahedralCuspedCensus import *
>>> M=TetrahedralOrientableCuspedCensus['otet02_0000'] # also m003
>>> TetrahedralOrientableCuspedCensus.identify(Manifold('m004'))
otet02_0001(0,0)
>>> len(TetrahedralOrientableCuspedCensus(tets=5)) # Number with 5 tets
2
>>> for M in TetrahedralOrientableCuspedCensus(tets=5):
...     print OrientableCuspedCensus.identify(M)
m410(0,0)
m412(0,0)(0,0)
>>> TetrahedralOrientableCuspedCensus.identify(Manifold("m208"))
>>>
```

The last example shows that `m208` is not a tetrahedral manifold since it has only 5 tetrahedra and thus would be in the tetrahedral census. Note that `SnapPy`'s `is_isometric_to` is using numerical methods and can fail to find an isomorphism. To verify that `m208` is not tetrahedral, one can certify its isometry signature[2] and check that it is not in the data files [Goerner 15b] provided with this paper.

4.3. Regina files

We also provide the census of combinatorial tetrahedral tessellations as two `Regina` files (for orientable and non-orientable) in the `Regina` directory accompanying this article. Each file groups the combinatorial tetrahedral tessellations first by number of tetrahedra and then by isometry class. The container for each isometry class contains the different combinatorial tetrahedral tessellations as well as the canonical retriangulation.

The `Regina` files can be inspected using the `Regina` GUI or the `Regina` python API. An example of how to traverse the tree structure in the file is given in `regina/example.py`.

4.4. Morphisms

Similarly to combinatorial isomorphism, we can define a *combinatorial homomorphism* between combinatorial tetrahedral tessellations, but without the requirement that different tetrahedra in the source go to the different tetrahedra in the destination. It assigns to each tetrahedron in the source a tetrahedron in the destination and a permutation in S_4 indicating which vertex of the source tetrahedron is mapped to which vertex of the destination tetrahedron. These permutations have to be compatible with the gluings of the source and destination tetrahedra. If the tessellations are connected and have no open faces, the source triangulation needs to have the same number of or a multiple of the number of tetrahedra as the destination. Topologically, a combinatorial homomorphism is a covering map that preserves the triangulation. We have implemented a procedure to list all combinatorial homomorphisms for a pair of triangulations in python.

We give a list of all pairs (M, N) of combinatorial tetrahedral tessellations such that there is a combinatorial homomorphism from M to N as a text file `data/morphisms.txt`. We do not include the trivial pairs (M, M) or pairs (M, N) which factor through another combinatorial tetrahedral tessellation as those can be recovered trivially through the reflexive and transitive closure. We also give some of the resulting graphs in `misc/graphs`. We discuss an example in more detail later in Section 5.3.

[2] We plan a future publication describing how to generalize the techniques for certifying isometry signatures to all cusped hyperbolic manifolds. The third named author has already incorporated this into SnapPy, beginning with version 2.3.2, see SnapPy documentation.

5. Properties of tetrahedral manifolds

5.1. Tetrahedral manifolds are arithmetic

Recall that two manifolds (or orbifolds) are commensurable if they have a common finite cover. Commensurability is an equivalence relation. The commensurability class of the figure-eight knot complement `m004` consists exactly of the cusped hyperbolic orbifolds and manifolds with invariant trace field $\mathbb{Q}(\sqrt{-3})$ that are arithmetic or, equivalently, that have integral traces [Maclachlan and Reid 03, Theorems 8.2.3 and 8.3.2]. Thus, tetrahedral manifolds are also arithmetic with the same invariant trace field since

Lemma 5.1. *Tetrahedral manifolds are commensurable to* `m004`*.*

More precisely, the commensurability class of `m004` also contains the orbifold $\mathfrak{R} = \mathbb{H}^3/\mathrm{Isom}(\{3, 3, 6\})$ where the Coxeter group $\mathrm{Isom}(\{3, 3, 6\})$ is the symmetry group of the regular tessellation $\{3, 3, 6\}$ by regular ideal tetrahedra. This orbifold can be used to characterize the tetrahedral manifolds in this commensurability class:

Lemma 5.2. *A manifold M is a covering space of $\mathfrak{R}$ if and only if it is tetrahedral.*

Proof. A combinatorial tetrahedral tessellation of a manifold M lifts to the tessellation $\{3, 3, 6\}$ in its universal cover $\mathbb{H}^3$. Thus, $\pi_1(M)$ is a subgroup of the symmetry group $\mathrm{Isom}(\{3, 3, 6\})$. Consequently, M is a cover of $\mathfrak{R}$.

Conversely, a covering map $M \to \mathfrak{R}$ induces a combinatorial tetrahedral tessellation on the manifold M with the standard fundamental domain of $\mathfrak{R}$ lifting to the barycentric subdivision of the combinatorial tetrahedral tessellation. □

5.2. Implications of the Margulis Theorem

Since `m004` is arithmetic, Margulis Theorem implies that its commensurator is not discrete and thus the commensurability class of `m004` contains no minimal element (with respect to covering) [Neumann and Reid 92a, Maclachlan and Reid 03, Walsh 11]. In particular, $\mathfrak{R}$ is not the minimal element of the commensurability class. We thus expect to see the following phenomena in the commensurability class containing the tetrahedral manifolds:

- Non-tetrahedral manifolds that are still commensurable with `m004`. For example, the following manifolds in SnapPy's `OrientableCuspedCensus` up to 8 simplices have this property:

  `m208`, `s118`, `s119`, `s594`, `s595`, `s596`, `v2873`, `v2874`.
- Tetrahedral manifolds M with different covering maps $M \to \mathfrak{R}$ inducing non-isomorphic combinatorial tetrahedral tessellations of the same manifold M.
- Combinatorial tetrahedral tessellations "hiding symmetries," defined as follows.

Definition 5.3. A combinatorial tetrahedral tessellation T hides symmetries if the corresponding tetrahedral manifold M has an isometry that is not induced from a combinatorial automorphism of T. In other words, if there is an isometry $M \to M$ that does not commute with the covering map $M \to \mathfrak{R}$ corresponding to T.

In this section, we will illustrate these phenomena using the tetrahedral census.

Remark 5.4. By definition, the canonical cell decomposition and thus the canonical retriangulation sees all isometries, so we can detect this by checking that the number of combinatorial automorphisms of the canonical retriangulation is higher than those of the combinatorial tetrahedral tessellation. To enable the reader to do this, the Regina file containing the tetrahedral census [Goerner 15b] includes the canonical retriangulation as well. The combinatorial automorphisms can be found using the method `findAllIsomorphisms` of a Regina triangulation or `find_morphisms` in `src/morphismMethods.py`.

Remark 5.5. The minimum volume orientable cusped hyperbolic orbifold $\mathfrak{M} = \mathbb{H}^3/\mathrm{PGL}(2, \mathbb{Z}[\zeta])$ and the Bianchi orbifold $\mathfrak{B} = \mathbb{H}^3/\mathrm{PSL}(2, \mathbb{Z}[\zeta])$ of discriminant $D = -3$ where $\zeta = \frac{1+\sqrt{-3}}{2}$ are related to $\mathfrak{R}$ as follows with each map being a 2-fold covering [Neumann and Reid 92b]:

$$\mathfrak{B} \to \mathfrak{M} \to \mathfrak{R}.$$

Similarly to $\mathfrak{R}$ being the quotient of $\mathbb{H}^3$ by the symmetry group of the regular tessellation $\{3, 3, 6\}$, $\mathfrak{M}$ corresponds to orientation-preserving symmetries, and $\mathfrak{B}$ corresponds to the symmetry group of the regular tessellation $\{3, 3, 6\}$ after two-coloring the regular ideal tetrahedra.

Thus, the manifold covering spaces of $\mathfrak{M}$ correspond to the orientable combinatorial tetrahedral tessellations, and the manifold covering spaces of $\mathfrak{B}$ correspond to orientable combinatorial tetrahedral tessellations whose tetrahedra can be two-colored. Regina displays the dual 1-skeleton of a triangulation in its UI under "Skeleton: face pairing graph," so we can check whether a combinatorial tetrahedral tessellation is a cover of $\mathfrak{B}$ by testing whether the graph Regina shows is two-colorable. For example, all orientable combinatorial tetrahedral tessellations with fewer than 5 tetrahedra are covers of $\mathfrak{B}$. But $\mathrm{otet05}_{0000}$ and $\mathrm{otet06}_{0000}$ are not.

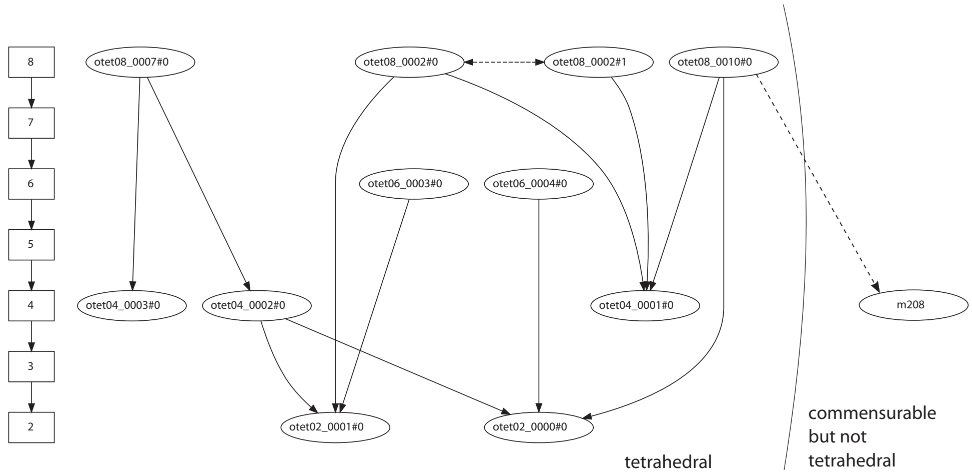

Figure 2. A small part of the category $\mathcal{T}$ of combinatorial tetrahedral tessellations (solid arrows) and the larger category $\mathcal{M}$ of manifolds commensurable with m004 (dashed arrows). Multiple morphisms between two objects are collapsed to just one arrow, automorphisms and morphisms factoring through another object are dropped.

Remark 5.6. Related results include: [Bowditch et al. 95] shows that all once-punctured torus bundles in the commensurability class of the figure eight-knot complement m004 are actually cyclic covers of the tetrahedral manifolds m003 and m004 and thus tetrahedral. The non-arithmetic hyperbolic once-punctured torus bundles are studied in [Goodman et al. 08] where an algorithm is given to compute the commensurator of a cusped non-arithmetic hyperbolic manifold. [Reni and Andrei 01] studies symmetries of or hidden by cyclic branched coverings of 2-bridge knots.

5.3. The category of combinatorial tetrahedral tessellations

To study the commensurability class containing the tetrahedral manifolds, we think of it as a category. For this, recall the notion of a combinatorial homomorphism from Section 4.4. On the underlying topological space, a combinatorial homomorphism is a covering map. We thus get two categories with a forgetful functor $\mathcal{T} \to \mathcal{M}$:

Definition 5.7. The *category $\mathcal{M}$ of manifolds commensurable with tetrahedral manifolds* has as objects manifolds commensurable with m004 and as morphisms covering maps.

The *category $\mathcal{T}$ of combinatorial tetrahedral tessellations* has as objects combinatorial tetrahedral tessellations and as morphisms combinatorial homomorphisms.

We show a small part of these categories in Figure 2 and observe:

- otet04_{0001}#0 has two 2-covers (indicated by the solid arrows) giving two different triangulations otet08_{0002}#0 and otet08_{0002}#1. These triangulations are not combinatorially isomorphic but yield isometric manifolds (indicated by the dashed line).
- The figure-eight knot complement, otet02_{0001}#0, and its sister, otet02_{0000}#0, have a common cover otet04_{0002}#0. More general, any two combinatorial tetrahedral tessellations have a common cover combinatorial tetrahedral tessellation as they are in the same commensurability class.
- otet02_{0001}#0 and otet02_{0000}#0 show that the graph is a poset with more than one minimal element. In fact, most combinatorial tetrahedral tessellations in our census are minimal elements and we conjecture that there are infinitely many such minimal elements.
- The figure also shows a manifold m208, which is non-tetrahedral. However, as with any manifold in this commensurability class, it still has a tetrahedral covering space, here otet08_{0010}#0 (the arrow has to be dashed because m208 is not tetrahedral so the map is not a combinatorial homomorphism).

Remark 5.8. The last example shows that the combinatorial tetrahedral tessellation otet08_{0010}#0 hides symmetries as in Definition 5.3. To see this, notice that the covering space otet08_{0010} $\to$ m208 is 2-fold, thus regular and m208 is the quotient of otet08_{0010} by the group $G = \mathbb{Z}/2\mathbb{Z}$ of deck transformations. If G preserved the combinatorial tetrahedral tessellation otet08_{0010}#0, the quotient m208 would have an induced combinatorial tetrahedral tessellation. But m208 is not tetrahedral, thus the nontrivial element of G is a symmetry of otet08_{0010}#0 which is not a combinatorial homomorphism.

5.4. Canonical cell decompositions

5.4.1. Examples

The canonical cell decomposition of a tetrahedral manifold can:

- Be a **combinatorial tetrahedral tessellation**.
  Examples: otet02_{0000} and otet10_{0010}. The latter one has two combinatorial tetrahedral tessellations, otet10_{0010}#0 being the canonical cell decomposition.
- Be a **coarsening** of a combinatorial tetrahedral tessellation.
  (I.e., the combinatorial tetrahedral tessellation is a subdivision of the canonical cell decomposition.)
  Example: otet05_{0001}. The canonical cell decomposition consist of single regular ideal cube that can be subdivided into 5 tetrahedra (see Figure 1) such that the diagonals introduced on the faces are compatible. This yields the unique (up to combinatorial isomorphism) combinatorial tetrahedral tessellation for this manifold. We elaborate on the relationships to cubes below.
- **Neither** of the above.
  In which case, the canonical cell decomposition can still
  - Consists of (non-regular) tetrahedra.
    Example: otet08_{0010}.
  - Contain cells which are not tetrahedra.
    Example: otet08_{0001}. Its canonical cell decomposition contains some hexahedra obtained by gluing two non-regular tetrahedra.

5.4.2. Cubical manifolds

Recall from Remark 3.7 that a manifold was called cubical if it can be decomposed into regular ideal cubes. Figure 1 showed that there are two choices of picking alternating vertices of a cube, which span a tetrahedron and thus yield a subdivision of a regular ideal cube into 5 regular ideal tetrahedra. Even though each cube of a combinatorial cubical tessellation can be subdivided into regular ideal tetrahedra individually, this only yields a combinatorial tetrahedral tessellation if the choices made are compatible with the face-pairings of the combinatorial cubical tessellation. We saw otet05_{0001} above as an example where this was possible and `x103` in Remark 3.7 as an example where this was impossible.

If a manifold is both tetrahedral and cubical, the canonical cell decomposition can actually consist of regular cubes or regular ideal tetrahedra (or neither). This is illustrated by the two cubical links given by Aitchison and Rubinstein [Aitchison and Rubinstein 92]:

- The canonical cell decomposition of the complement otet10_{0011} of the alternating 4-chain link `L8a21` (see Figure 3) consists of two regular ideal cubes.
- The complement otet10_{0006} of the other cubical link `L8a20` (see Figure 3) admits two combinatorial tetrahedral tessellations up to combinatorial isomorphism, one of which is equal to the canonical cell decomposition.

Remark 5.9. Figure 1 also shows that the choice of 5 regular ideal tetrahedra to subdivide a cube hides symmetries of the cube, namely, the rotation by $\pi/2$ of the cube that takes one choice to the other. This rotation is an element in the commensurator but not in the normalizer of Isom($\{3, 3, 6\}$) and thus a hidden symmetry of $\mathfrak{N}$. A combinatorial tetrahedral tessellation arising as subdivision of a combinatorial cubical tessellation can hide the symmetries of the combinatorial cubical tessellation corresponding to this rotation, i.e., there can be symmetries of the combinatorial cubical tessellation that are not symmetries of the combinatorial tetrahedral tessellation.

An example of this is otet10_{0011}. Other examples are obtained by subdividing the cubical regular tessellation link complements $\mathcal{U}^{\{4,3,6\}}_{1+\zeta}$, $\mathcal{U}^{\{4,3,6\}}_{2}$, and $\mathcal{U}^{\{4,3,6\}}_{2+\zeta}$ classified in [Goerner 15a]. By definition, each of these three manifolds can be decomposed into ideal regular cubes such that each flag of a cube, an adjacent face and an edge adjacent to the face can be taken to any other flag by a symmetry. In particular, these manifolds contain a symmetry flipping the diagonals of the faces of the cubes.

5.4.3. Canonical combinatorial tetrahedral tessellations

We call a combinatorial tetrahedral tessellation a regular tessellation if it corresponds to a regular covering space of $\mathfrak{N}$ or $\mathfrak{M}$. This is equivalent to saying that the combinatorial automorphisms act transitively on flags consisting of a tetrahedron, an adjacent face and an adjacent edge (we drop the vertex in the flag to allow chiral combinatorial tetrahedral tessellations) [Goerner 15a].

Lemma 5.10. *Consider a combinatorial tetrahedral tessellation T. T is equal to the canonical cell decomposition of the corresponding tetrahedral manifold M if T is a regular tessellation or if M has only one cusp. In particular, a tetrahedral manifold with only one cusp has a unique combinatorial tetrahedral tessellation. If T is equal to the canonical cell decomposition, then T hides no symmetries.*

Proof. Recall from Section 3.1 that the canonical cell decomposition relies on choosing cusp neighborhoods of the same volume for each cusp. If T is regular, then each cusp neighborhood intersects T in the same triangulation. This is also true if M has only one cusp and there is only one cusp neighborhood to choose. Thus, each end

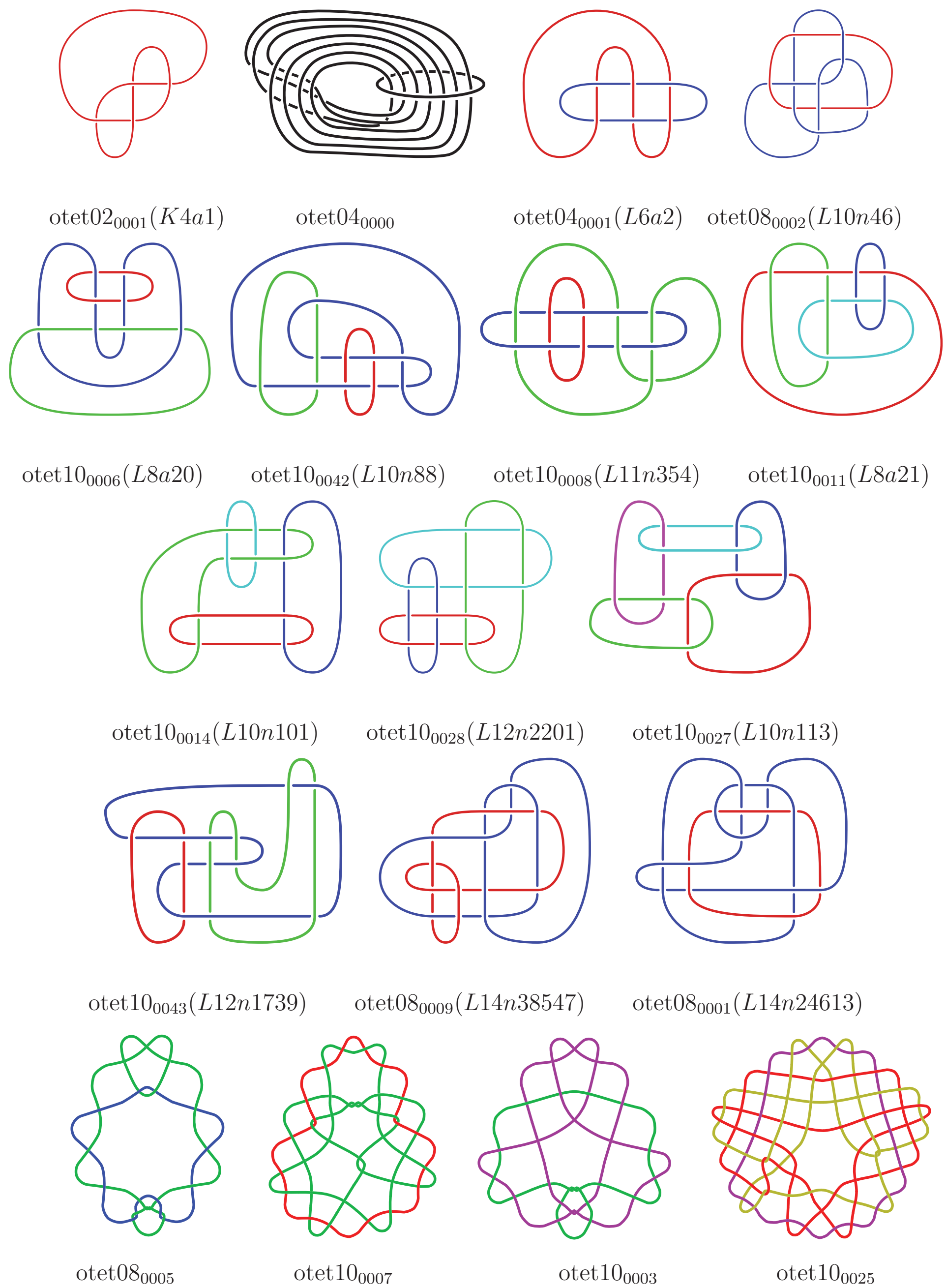

Figure 3. The tetrahedral links with at most 10 tetrahedra.

of a tetrahedron intersects the cusp neighborhoods in the same volume. T lifts to the regular tessellation {3, 3, 6} of $\mathbb{H}^3$ and the cusp neighborhoods lift to horoballs with the same symmetry. Hence, the canonical cell decomposition is equal to T. The other statement follows from the canonical cell decomposition not hiding any symmetries by definition. □

Remark 5.11. For some cubical tessellations such as $\mathcal{U}_{1+\zeta}^{\{4,3,6\}}$, $\mathcal{U}_{2}^{\{4,3,6\}}$, and $\mathcal{U}_{2+\zeta}^{\{4,3,6\}}$, we can partition the cusps into two disjoint sets such that no edge connects two cusps of the same set. If, in the construction of the canonical cell decomposition, we now pick for cusps in one set cusp neighborhoods of a volume slightly different from those for cusps in the other set, we no longer obtain the cubical tessellation but one of the two subdivided combinatorial tetrahedral tessellations depending on which set of cusps we favored.

6. Tetrahedral links

6.1. Some facts about tetrahedral links

Consider a cusped 3-manifold M, i.e., the interior of a compact 3-manifold $\bar{M}$ with boundary $\partial\bar{M}$ a disjoint union of tori. We say that M is a *homology link complement* if the long exact sequence in homology associated

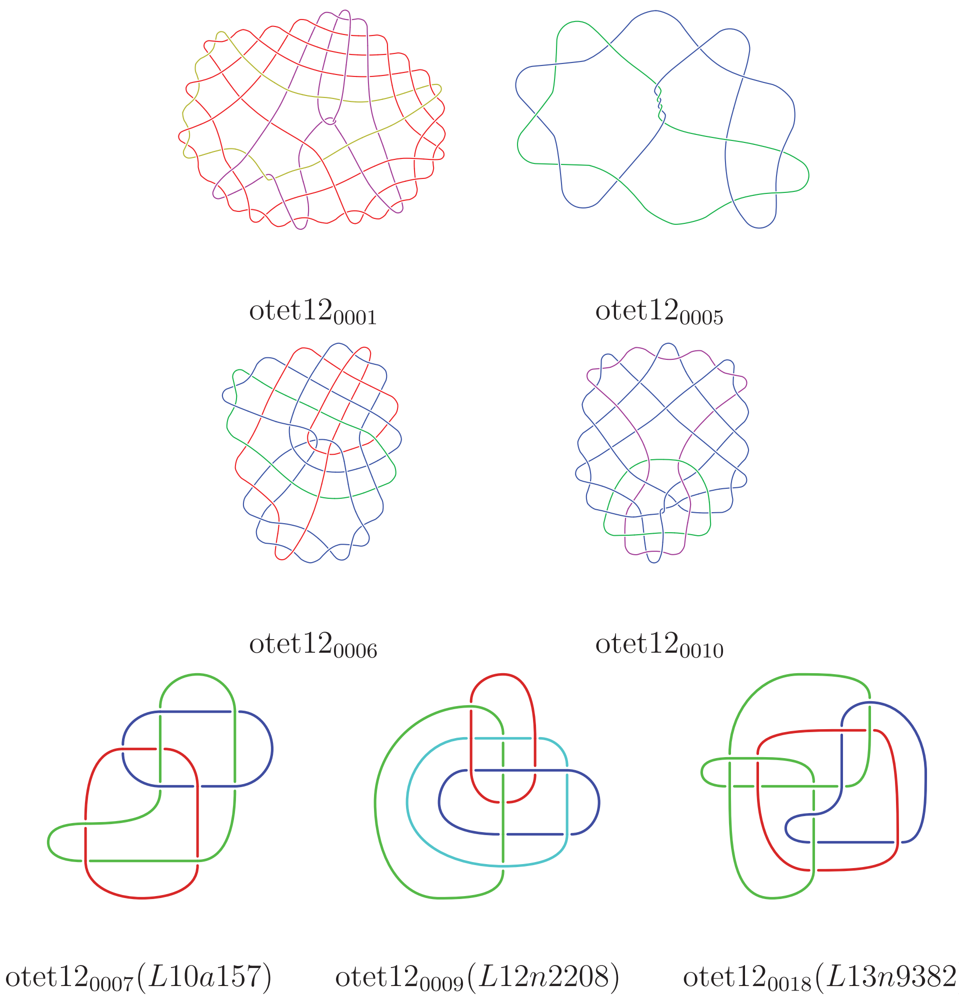

Figure 4. The tetrahedral links with 12 tetrahedra.

to $(\bar{M}, \partial\bar{M})$ is isomorphic to that of the complement of a link in S^3. Let $i : \partial\bar{M} \to \bar{M}$ denote the inclusion of the boundary. We thank C. Gordon for pointing out to us that (b) implies (d).

Lemma 6.1. *Let M be a cusped 3-manifold. The following are equivalent:*

(a) M is a homology link complement.
(b) $H_1(M; \mathbb{Z}) = \mathbb{Z}^c$ where c is the number of cusps.
(c) The cuspidal homology $H_1^{\mathrm{cusp}}(M) = H_1(\bar{M}; \mathbb{Z})/\mathrm{Im}(i_*)$ vanishes.
(d) M is the complement of a link in an integral homology sphere.

Proof. (a) implies (b) since $H_1(\partial\bar{M}) \cong \mathbb{Z}^{2c}$ determines c and $H_1(M) = \mathbb{Z}^c$ for a link complement in S^3. The equivalence of (b) and (c) was shown in [Goerner 15a, Lem.6.9]. To prove that (b) implies (d), we work by induction on c. For $c = 0$, M is a homology sphere and thus the complement of the empty link. Assuming it is true for $c - 1$, pick a component T of $\partial\bar{M}$ and let H be the image of $H_1(T; \mathbb{Z})$ in $H_1(\bar{M}; \mathbb{Z})$ under the map induced by inclusion. By Poincare duality, H has rank 1 or 2 (apply [Bredon 97, Chapter VI, Theorem 10.4] to $\bar{M}$ with all boundary components but T Dehn-filled). Now we claim that H contains a rank 1 direct summand of $H_1(\bar{M}; \mathbb{Z})$ (so one can now do a Dehn filling on T to reduce c by 1). For if not, then H is contained in $pH_1(\bar{M}; \mathbb{Z})$ for some prime p. Then $H_1(T; \mathbb{Z}_p)$ maps trivially in $H_1(\bar{M}; \mathbb{Z}_p)$, contradicting duality.

It is left to show that (d) implies (a). This follows easily from Alexander duality [Burde and Zieschang 85]. □

A homology link M is the complement of a link in the 3-sphere if and only if there is a Dehn-filling of it with trivial fundamental group. In that case, the filling is a homotopy 3-sphere, hence a standard 3-sphere (by Perelman's Theorem), and the link is the complement of the core of the filling. `SnapPy` can compute the homology of a hyperbolic manifold as well as a presentation of its fundamental group, before or after filling. Note that links are in general not determined by their complement, i.e., there are 3-manifolds that arise as the complement of infinitely

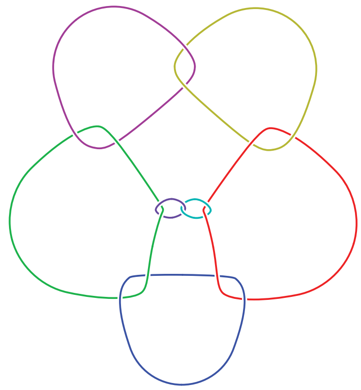

Figure 5. The remarkable link otet20_{0570}.

many different links [Gordon and Luecke 89]. On the other hand, the only tetrahedral knot is the figure-eight knot. This follows from the fact that tetrahedral manifolds are arithmetic, and the only arithmetic knot is the figure-eight knot [Reid 91, Theorem 2].

6.2. A list of tetrahedral links

Of the 124 orientable tetrahedral manifolds with at most 12 tetrahedra, 27 are homology links and `SnapPy` identified 13 of them with link exteriors in its census. Of the remaining 14 homology links,

- otet04_{0000} is the Berge manifold, the complement of a link in [Martelli and Petronio 06],
- 11 are link complements, with corresponding links shown in Figures 3 and 4.
  (These links were found by drilling some curves until the manifold could be identified as a complement of a link in SnapPy's `HTLinkExteriors`. We then found a framing of some components of the link such that Dehn-filling gives back the tetrahedral manifold. This gives us a Kirby diagram of the tetrahedral manifold. Using the Kirby Calculator [Swenton 14], we successfully removed all Dehn-surgeries and obtained a link.)
- otet08_{0003} and otet10_{0023} (with 2 and 1 cusps, respectively) are not link complements.
  (This can be shown using `fef_gen.py` based on [Martelli et al. 14] and available from [Ichihara and Masai 14] to list all exceptional slopes and then compute homologies for those.)

The data in Table 1 also suggest:

Conjecture 6.2. Every tetrahedral link complement has an even number of tetrahedra (i.e., a corresponding combinatorial tetrahedral tessellation has an even number of tetrahedra).

6.3. A remarkable tetrahedral link

Of the 11,580 orientable tetrahedral manifolds with at most 25 tetrahedra, 885 are homology links, and have at most 7 cusps. There is a unique tetrahedral manifold with 7 cusps, otet20_{0570}, which is a link complement, and a 2-fold cover of the minimally twisted 5-chain link $L10n113$ = otet10_{0027}. This remarkable link is shown in Figure 5.

Acknowledgments

We would like to thank Frank Swenton for adding the features to the Kirby calculator [Swenton 14] necessary to draw the new tetrahedral links, and Cameron Gordon for completing the proof of Lemma 6.1.

Funding

E.F., V.T., and A.V. were supported in part by the Ministry of Education and Science of the Russia (the state task number 1.1260.2014/K) and RFBR grant 16-01-00414. S.G. was supported in part by a National Science Foundation grant DMS-14-06419. M.G. was supported in part by a National Science Foundation grant DMS-11-07452.

References

[Aitchison and Rubinstein 92] I. R. Aitchison and J. H. Rubinstein. "Combinatorial Cubings, Cusps, and the Dodecahedral Knots." In *Topology '90 (Columbus, OH, 1990)*. Ohio State Univ. Math. Res. Inst. Publ., vol. 1, edited by Boris N. Apanasov, Walter D. Neumann, Alan W. Reid, and Laurent Siebenmann, pp. 17–26. Berlin: de Gruyter, 1992.

[Anisov 05] S. Anisov. "Exact Values of Complexity for an Infinite Number of 3-Manifolds." *Moscow Math. J.* 5:2 (2005), 305–310.

[Bowditch et al. 95] B. H. Bowditch, C. Maclachlan, and A. W. Reid. "Arithmetic Hyperbolic Surface Bundles." *Math. Ann.* 302:1 (1995), 31–60.

[Bredon 97] Glen E. Bredon. *Topology and Geometry*. Graduate Texts in Mathematics, vol. 139. New York, NY: Springer-Verlag, 1997. Corrected third printing of the 1993 original.

[Burde and Zieschang 85] Gerhard Burde and Heiner Zieschang. *Knots*. de Gruyter Studies in Mathematics, vol. 5. Berlin: Walter de Gruyter & Co., 1985.

[Burton 11] Benjamin A. Burton. "The Pachner Graph and the Simplification of 3-Sphere Triangulations." In *Computational Geometry (SCG'11)*, pp. 153–162. New York, NY: ACM, 2011. arXiv:1110.6080.

[Burton 14] Benjamin Burton. "Regina, Software for 3-Manifold Topology and Normal Surface Theory." Available at http://regina.sourceforge.net, January 2014.

[Burton 14] Benjamin A. Burton. "A Duplicate Pair in the SnapPea Census." *Exp. Math.* 23:2 (2014), 170–173.

[Burton and Pettersson 14] Benjamin A. Burton and William Pettersson. "An Edge-Based Framework for Enumerating 3-Manifold Triangulations." Preprint, arXiv:1412.2169, 2014.

[Callahan et al. 99] Patrick J. Callahan, Martin V. Hildebrand, and Jeffrey R. Weeks. "A Census of Cusped Hyperbolic

3-Manifolds." *Math. Comp.* 68:225 (1999), 321–332. With microfiche supplement.

[Culler et al. 14] Marc Culler, Nathan M. Dunfield, and Jeffrey R. Weeks. "SnapPy, a Computer Program for Studying the Topology of 3-Manifolds." Available at http://snappy.computop.org, January 2014.

[Dunfield et al. 14] Nathan M. Dunfield, Neil R. Hoffman, and Joan E. Licata. "Asymmetric Hyperbolic L-Spaces, Heegaard Genus, and Dehn Filling." Preprint, arXiv:1407.7827, 2014.

[Epstein and Penner 88] D. B. A. Epstein and R. C. Penner. "Euclidean Decompositions of Noncompact Hyperbolic Manifolds." *J. Differential Geom.* 27:1 (1988), 67–80.

[Goerner 15a] Matthias Goerner. "Regular Tessellation Link Complements." *Exp. Math.* 24:2 (2015), 225–246. Available online http://arxiv.org/abs/1406.2827.

[Goerner 15b] Matthias Goerner. "A Census of Tetrahedral Hyperbolic Manifolds." Available online http://unhyperbolic.org/tetrahedralCensus/, 2015.

[Goodman et al. 08] Oliver Goodman, Damian Heard, and Craig Hodgson. "Commensurators of Cusped Hyperbolic Manifolds." *Exp. Math.* 17:3 (2008), 283–306.

[Gordon and Luecke 89] C. McA. Gordon and J. Luecke. "Knots are Determined by Their Complements." *J. Am. Math. Soc.* 2:2 (1989), 371–415.

[Hoffman et al. 13] N. Hoffman, K. Ichihara, M. Kashiwagi, H. Masai, S. Oishi, and A. Takayasu. "Verified Computations for Hyperbolic 3-Manifolds." arXiv:1310.3410. Available online http://www.oishi.info.waseda.ac.jp/˜takayasu/hikmot, 2013.

[Ichihara and Masai 14] K. Ichihara and H. Masai. `fef_gen.py`, http://www.math.chs.nihon-u.ac.jp/˜ichihara/ExcAlt/, 2014.

[Lang 02] Serge Lang. *Algebra*. Graduate Texts in Mathematics, vol. 211, third edition. New York, NY: Springer-Verlag, 2002.

[Luo et al. 08] Feng Luo, Saul Schleimer, and Stephan Tillmann. "Geodesic Ideal Triangulations Exist Virtually." *Proc. Am. Math. Soc.* 136:7 (2008), 2625–2630.

[Maclachlan and Reid 03] Colin Maclachlan and Alan W. Reid. *The Arithmetic of Hyperbolic 3-Manifolds*. Graduate Texts in Mathematics, vol. 219. New York, NY: Springer-Verlag, 2003.

[Martelli and Petronio 06] Bruno Martelli and Carlo Petronio. "Dehn Filling of the "Magic" 3-Manifold." *Commun. Anal. Geom.* 14:5 (2006), 969–1026.

[Martelli et al. 14] Bruno Martelli, Carlo Petronio, and Fionntan Roukema. "Exceptional Dehn Surgery on the Minimally Twisted Five-Chain Link." *Commun. Anal. Geom.* 22:4 (2014), 689–735.

[Matveev 03] Sergei Matveev. *Algorithmic Topology and Classification of 3-Manifolds*. Algorithms and Computation in Mathematics, vol. 9. Berlin: Springer-Verlag, 2003.

[Neumann and Reid 92a] Walter D. Neumann and Alan W. Reid. "Arithmetic of Hyperbolic Manifolds." In *Topology '90 (Columbus, OH, 1990)*. Ohio State Univ. Math. Res. Inst. Publ., vol. 1, edited by Boris N. Apanasov, Walter D. Neumann, Alan W. Reid, and Laurent Siebenmann, pp. 273–310. Berlin: de Gruyter, 1992.

[Neumann and Reid 92b] Walter D. Neumann and Alan W. Reid. "Notes on Adams' Small Volume Orbifolds." In *Topology '90 (Columbus, OH, 1990)*. Ohio State Univ. Math. Res. Inst. Publ., vol. 1, edited by Boris N. Apanasov, Walter D. Neumann, Alan W. Reid, and Laurent Siebenmann, pp. 311–314. Berlin: de Gruyter, 1992.

[Petronio and Weeks 00] Carlo Petronio and Jeffrey R. Weeks. "Partially Flat Ideal Triangulations of Cusped Hyperbolic 3-Manifolds." *Osaka J. Math.* 37:2 (2000), 453–466.

[Reid 91] Alan W. Reid. "Arithmeticity of Knot Complements." *J. Lond. Math. Soc. (2)* 43:1 (1991), 171–184.

[Reni and Andrei 01] Marco Reni and Vesnin Andrei. "Hidden Symmetries of Cyclic Branched Coverings of 2-Bridge Knots." *Rend. Istit. Mat. Univ. Trieste* XXXII (2001), 289–304.

[Swenton 14] Frank Swenton. "Kurby Calculator." Available online http://community.middlebury.edu/˜mathanimations/kirbycalculator/, 2014.

[Vesnin et al. 11] A. Yu. Vesnin, S. V. Matveev, and E. A. Fominykh. "Complexity of Three-Dimensional Manifolds: Exact Values and Estimates (in Russian)." *Sib. Èlektron. Mat. Izv.* 8 (2011), 341–364.

[Vesnin et al. 14] A. Yu. Vesnin, V. V. Tarkaev, and E. A. Fominykh. "On the Complexity of Three-Dimensional Cusped Hyperbolic Manifolds." *Doklady Math.* 89:3 (2014), 267–270.

[Vesnin et al. 15] A. Yu. Vesnin, V. V. Tarkaev, and E. A. Fominykh. "Three-Dimensional Hyperbolic Manifolds with Cusps of Complexity 10 Having Maximal Volume." *Proceedings of the Steklov Institute of Mathematics* 289 Suppl. 1 (2015), S227–S239.

[Walsh 11] Genevieve S. Walsh. *Orbifolds and Commensurability, Interactions between Hyperbolic Geometry, Quantum Topology and Number Theory*. Contemp. Math., vol. 541, pp. 221–231. Providence, RI: American Mathematical Society, 2011.

[Weeks 93] Jeffrey R. Weeks. "Convex Hulls and Isometries of Cusped Hyperbolic 3-Manifolds." *Topol. Appl.* 52:2 (1993), 127–149.